Influence of electrodes area ratios and the discharge volume in RF capacitively coupled plasma

Moyad Abdullah Ahmad

Department of Physics, College of Education, Mosul University, Iraq

E-mail: mouad68@yahoo.com

Abstract

Experimental results on harmonic distortions in 13.56 MHz RF Argon glow discharge using different grounded electrodes areas and electrodes spacing are presented. The experiment is carried out at four pressure values. RF power values used are between 20 and 90 watts. The results indicate significant increase in distortions at two specific values of the cone angle enclosing the two electrodes within its geometrical volume. The computation of the cone head angle gave the symmetry discharge or asymmetry as well as when the angle is small the condition is near symmetry discharge associated with decrease in the nonlinearity.

Key words
plasma, DC bias, Distortion.

Article info
Received: Sep. 2012
Accepted: Nov. 2012
Published: Apr. 2013

تأثير نسب مساحة الأقطاب و حجم التفريغ في البلازما الراديوية السعوية

مؤيد عبدالله احمد

قسم الفيزياء، كلية التربية، جامعة الموصل، العراق

الخلاصة

تم تعين النتائج التجريبية للتشوهات التوافقية في التفريغ الراديوي عند التردد 13.56MHz باستعمال مساحات مختلفة من الأقطاب المؤرضة عند مسافات مختلفة بين أقطاب التفريغ. نفذت التجربة عند أربعة قيم للضغوط. قيم القدرة الراديوية المستعملة بين (90–20) واط. تشير النتائج إلى زيادة واضحة في التشوهات عند قيمتين معينتين لزاوية رأس المخروط الذي يحتوي حجمه القطبين. حساب زاوية رأس المخروط أعطت التفريغ المتناظر أو التفريغ غير المتناظر فضلا عن ذلك عندما تكون الزاوية صغيرة الحالة تقترب من حالة التفريغ المتناظر مع انخفاض الحالة غير الخطية المرافقة.

Introduction

Low pressure, capacitively coupled radio discharge are widely used for material processing. capacitively coupled plasmas (CCPs) have been used for several decade for etching and deposition on the film [1, 2, 3, 4]. The CCP system, usually the geometry of RF discharge is very simple because design with two parallel electrodes. There are two type of CCPs RF discharge, symmetric discharge include two identical electrodes [5,6], whilst in asymmetric discharge systems the plasma formed between two unequal electrodes area, later create a dc voltage appears as a result for the

different in electron and ion mobility, this attributes to the different mass between them. Some research study the influence of the geometry design on the characteristics of CCP discharge with different gases as well as observed by using the different electrodes area ratio which play important role in dc-self bias [7-10]. Gottscho et al., [8] showed that the discharge structure in CCP system contains the layers sandwiches (sheath-plasma-sheath) usually formed with frequency well known 13.56 MHz in Argon plasma and the two sheaths at both of the two electrodes discharge can be described as a pure capacitive properties, in addition to this study gave very important results about the effects in the CCP discharge when using a different electrodes area ratio. In AC coupling connection the two sheaths can be described by the capacitive sheath model. In the case of a large, AC coupled driven (powered) electrode the DC bias (auto-bias) is positive, while in the case of a small driven electrode it is negative, but the absolute values are the same. This depend on the difference between the capacitor values due to the two sheaths at the two electrodes, this evidence by Raizer page (115) Eq.(3.6) [2]. Ahmad [11] used different grounded electrode surface areas and confirmed the increasing in the grounded electrode area plays important role in the CCPs discharge especially at the minimum breakdown in the Paschen curve in Argon gas. There is some experimental work on the harmonic properties of asymmetric RF discharge. Kawata et al.,[12] calculated the magnitude of second harmonic generated by plasma nonlinearity and they showed that it strongly dependent on the impedance plasma associated with the matching network circuit. Peter et al.,[13] investigated the harmonic and inter modulation distortion behavior of prototype plasma capacitor proposed for use as a radio frequency control device. Asmussen et al.,[14] presented and showed the effect of the capacitor size and input pump power on the parametric interaction. Dewan et al., [15] studied the harmonics which associated with the fundamental frequency in nonsymmetry (asymmetry) discharges in current wave and confirmed the most of the CCP discharges are asymmetry. Theoretical and modeling for symmetric and asymmetric RF discharges were presented by work on the generated harmonics. Lieberman [16] confirmed the scaling of potential with the current and showed that the current contains contribution up to the fourth harmonic in model includes two planar parallel plates. Lieberman [17] studied ion transport and bias voltage formation in asymmetric capacitive RF discharges, which have unequal electrode areas in spherical shell model. Barnes [18] used the simulation to compute the geometric factor for unequal electrode areas in CCP rf discharge 13.56MHz as a driven frequency. The different electrode area not only the unique way to obtain the dc self-biasing in the CCP system, but from symmetrical electrodes geometry driven by two consecutive harmonics represents the fundamental frequency 13.56 MHz, other one 27.12 MHz this discharge called dual frequency capacitively coupled radio frequency discharge (df ccrf) by using electric asymmetry effect (EAE) [19]. In the present work, the influence of the discharge parameters RF power, Argon gas pressure, inter-electrodes distance, the diameter (area) of grounded electrode, results current waveform distortion, DC-bias, second harmonic components are studied.

Experimental Apparatus

The experimental set up is shown in Fig.1. It involves a 20cm in height and 15cm inner diameter bell jar shaped glass discharge chamber with a Teflon flat base. Two circular flat well polished aluminum electrodes are installed inside the chamber.

The upper electrode is 12cm in diameter and fixed at the top. The lower electrode is changeable. A set of electrodes are prepared with diameters of 3, 4, 5 ,6,7, 8, 9, 10, 11, and 12cm are used as lower electrodes. A screw mechanism is used to change the distance between the upper and lower electrode in each case. Electrode separation used is 2.5, 3, 3.5, 4 and 4.5 cm with error ($\pm 1\ mm$). Both electrodes are insulated on the sides not facing the discharge. The rims of electrodes are also insulated (this achieved by machining a solid Teflon disk in a way such that the aluminum fits into machined region). The electrodes were subjected to several stages of polishing, washing with hydrochloric acid water, and acetone to remove any contaminants. Each electrode was further subjected to plasma cleaning by producing a discharge at low pressure of 1.5 Pa with 50 watts RF power for ten minutes to remove any remaining aluminum oxide layers from electrode surface. The chamber is connected to the vacuum pump, the gage valve, and the vacuum gauge via piping connections from the base side. The vacuum system involves Leybold Rotary Vane Vacuum Trivac D8b Rotary which has a nominal ultimate pressure 2×10^3 (0.27 Pa). The minimum base pressure reached 1Pa. The pressure is measured by a Leybold THERMOVAC transmitter model CAT.No.TTR91S connect to digital readout Leybold Vacuum model CAT.No.378514. The discharge is create using a 13.56 MHz RF generator (AMN 600 watt R Coaxial Power System) connected via an automatic impedance matching network. The current is measured by using a calibrated Rogowski coil (model GH3104-2 made by USR) surrounding the RF feed cable. The current signal produced by the Rogowski coil is applied to the Oscilloscope type HAMEG 100 MHz model 1004-3 HAMEG Instruments. Rogowski coil-oscilloscope system is calibrated. A digital picture is converted to numerical data using a special matlab image processing software [20].

Typical current signal containing distortions together with plot of numerical data retrieved are shown in Fig.2. Each time-current signal data set retrieved from the digital picture is analyzed using fast Fourier transformation to obtain the dc current, second harmonic components and the distortion which appears in the current signal. Typical result of such spectral analysis is also presented in Figs (2-c).

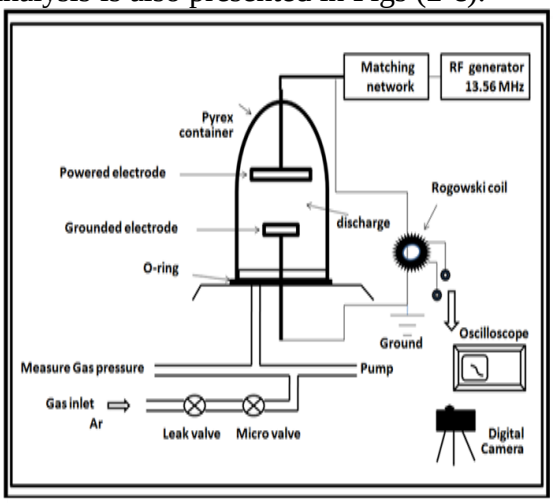

Fig.1: Experimental Set up

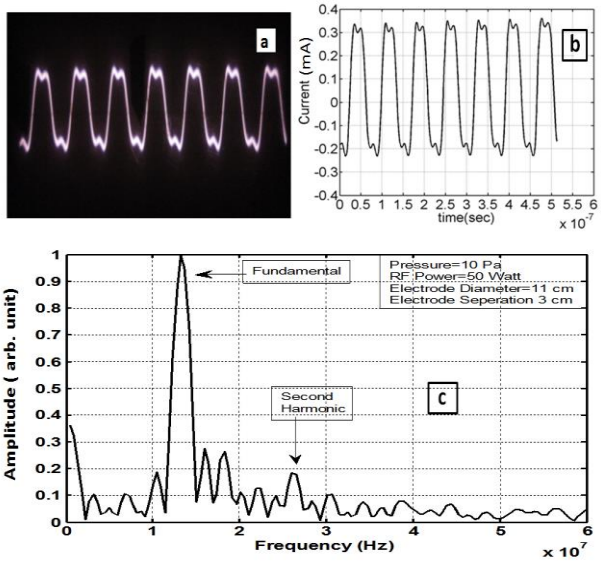

Fig.2: (a) Digital image of a typical current signal. (b) Plot of numerical data retrieved from picture in (a). (c) Frequency spectral analysis of the data in (b).

Result and Discussion

Due to the fact that the number of independent parameters is large pressure, electrodes spacing, electrodes area and RF power, it becomes slightly impractical to present the results on two dimensional plots. For this reason, three dimensional plots are preferred here. The distortion is computed for all the cases by Eq.(1), where the $Dist$ represents the ratio between the sum of all the harmonics amplitudes start from the second harmonic to infinity of the harmonics, that associated with the fundamental harmonic to the sum of all the amplitudes of the harmonics in addition to fundamental in the frequency spectral.

$$Dist = \left(\frac{\sum_{1}^{\infty} |A_{n+1}|^2}{\sum_{1}^{\infty} |A_n|^2} \right)^{1/2} \quad (1)$$

The distortion in the current wave comes from the nonlinearity which creates by the two sheaths near the two electrodes. When the area of the two electrodes are unequal and the ratio between the two electrodes area not equal one, this condition of CCP discharge usually called the asymmetric (nonsymmetric) discharge [2,4,15]. In the symmetry discharge the two sheaths are equal, due to equality of the areas ratio for the two electrodes are equal one, the influence of the nonlinearity which is generated by the sheath at one of the two electrodes, the other electrode will be generated the same effect but in the opposite direction [3,4,15].

Fig. 3 shows how can be computed of the cone head angle. The quantity $\tan\vartheta = (R-r)/h$ directly gives the angle of the head cone ϑ as in Eq. (2), where *R*, *r*, and *h* being the radii of the two electrodes and the distance between them respectively.

$$\vartheta = \tan^{-1}[(R-r)/h] \quad (2)$$

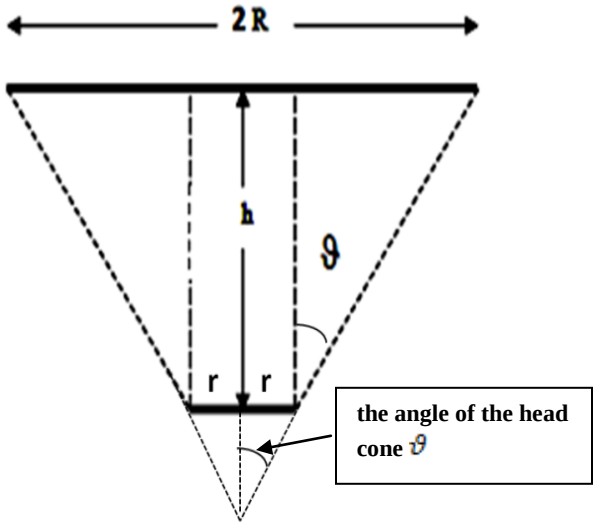

Fig.3: The schematic diagram of the plasma.

Fig. 4-a, b, c and d, Fig. 5-a, b, c and d and Fig. 6-a, b, c and d show the DC, second harmonic and distortion with the angle of the head cone and the RF power for the four pressures are used in the experiment. The indications from these plots, for the DC, second harmonic components and the distortion show that there are available regions higher than the other and their changes are very clear. The features of all the figures mentioned formerly above seem systematic.

The two plasma sheaths can be thought to be equivalent to two diodes with nonlinear I-V characteristics [21]. When the two electrodes are different in size, the corresponding diodes I-V characteristics will be different producing different responses to the applied voltage during each of the two half cycles of the RF field. This effect can be noticed in Fig. 2-a and b where the current signal at the upper half cycle is not a mirror of the lower half in addition to the fact that the whole signal is shifted upward.

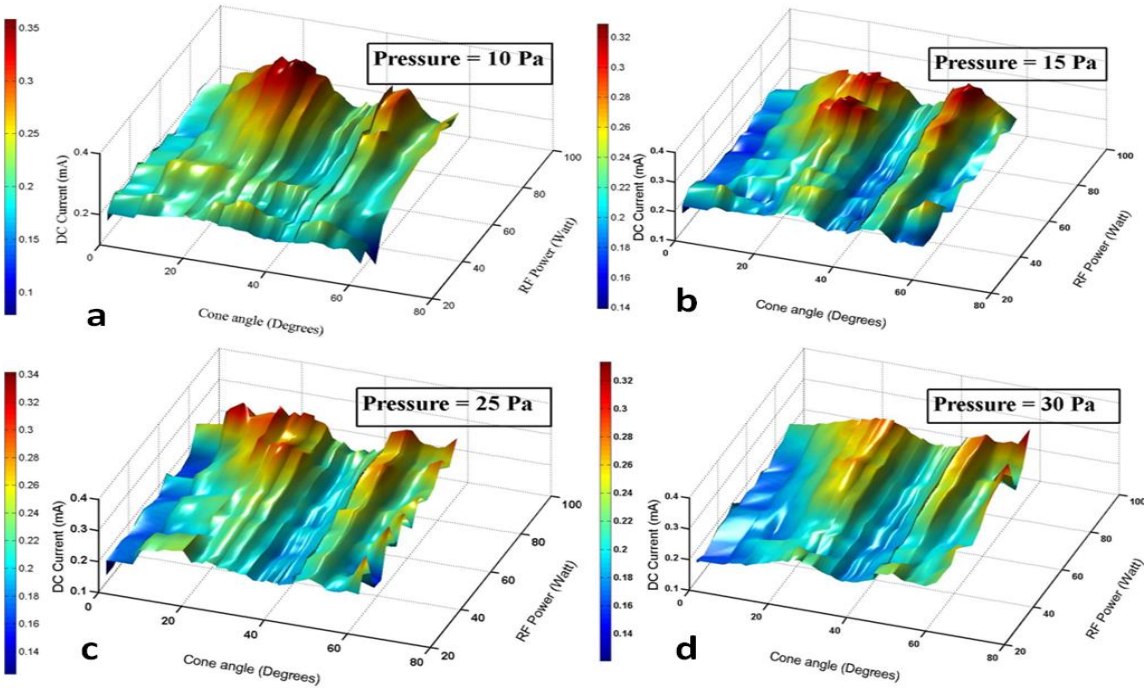

Fig.4: The DC component plotted against ϑ and RF power for four pressure values. a: 10 Pa, b: 15 Pa, c: 25 Pa, d: 30 Pa .

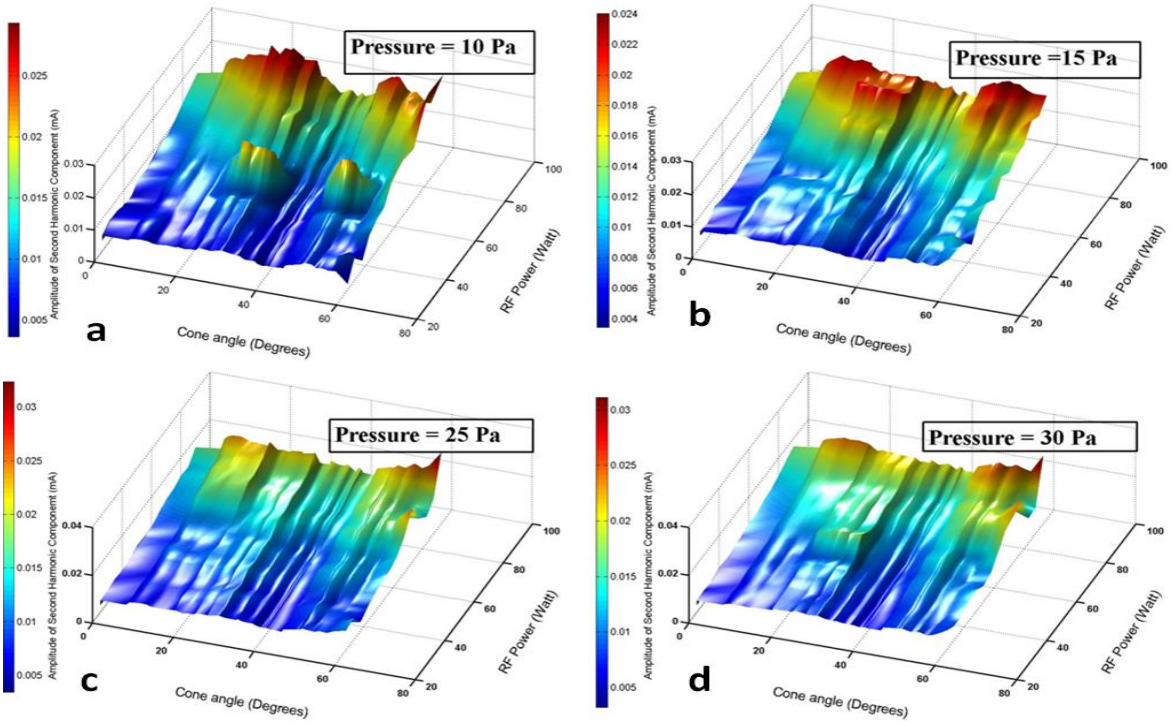

Fig.5: The second harmonic component plotted against ϑ and RF power for four pressure values. a: 10 Pa, b: 15 Pa, c: 25 Pa, d: 30 Pa .

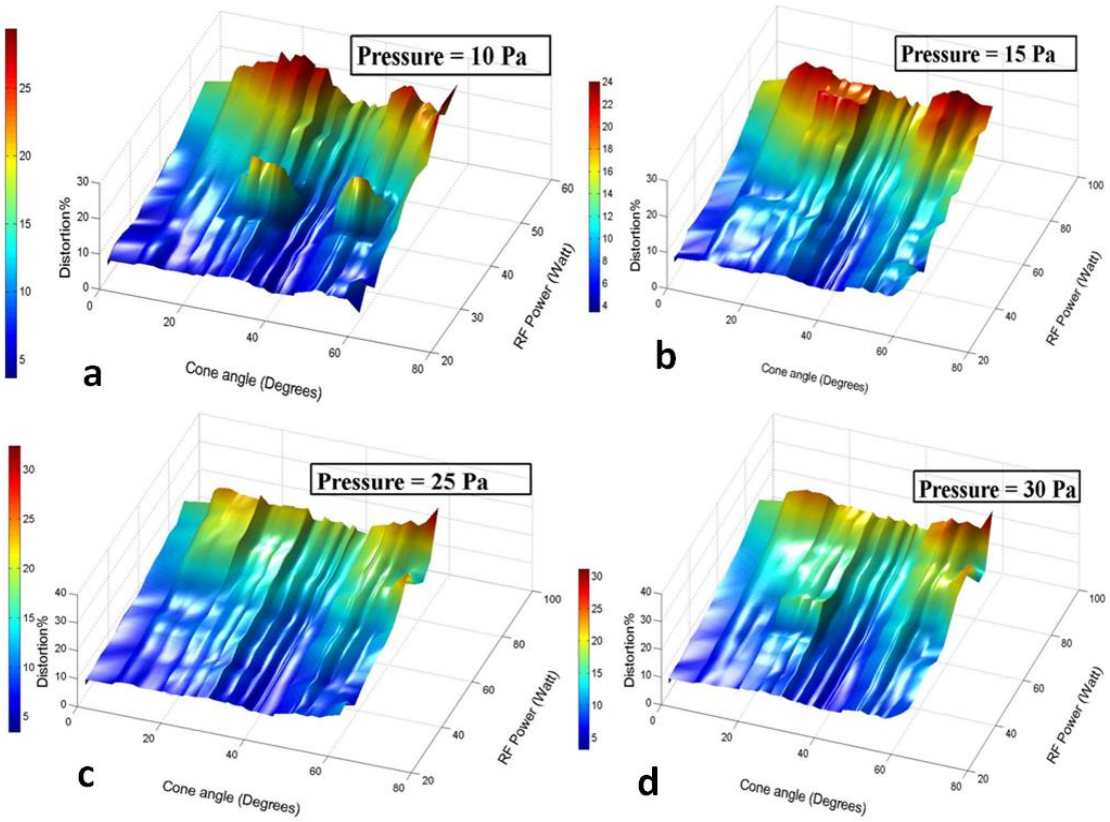

Fig.6: The distortion plotted against ϑ and RF power for four pressure values. a: 10 Pa, b: 15 Pa, c: 25 Pa, d: 30 Pa .

Few features can be noted from the Figs. 4, 5 and 6. The first: is that the general behavior of the DC, second harmonic and distortion contents are much similar. This indicates that the net DC bias is always associated with overall distortion of the current waveform associated with plasma nonlinearity. The second, which is the most important feature of the behaviors of these three quantities againstϑ, is the clear existence of the increase at two specific angles, the values of the first cone head angles around $15^{o}-30^{o}$ and the second around $45^{o}-55^{o}$. The third: the three components have a small values (when the discharge is electrically symmetric or the inter-electrodes distance is large) after that the values of these components increase with the increasing of the angle to reach high specific value at the range 15^{o} - 30^{o}. Therefore, there is a decreasing beyond this region after that the increase occurs in the range of the angle values 45^{o} - 55^{o}. These events are clear at all RF powers. The fourth: there are systematic increased for these components at all angles with increasing in RF power. The explanation for these cases can be demonstrated as follow:

When the cone head angle is small, this means there is a symmetry discharge (geometrical symmetry and electrical symmetry), the influence of the nonlinearity is generated by the sheath at one of the two electrodes, while the other electrode will be generated the same effect but in the opposite direction. As a result for this situation the DC bias will disappear [1]. When this angle increases to a specific value the inverse nonlinearity effects for both sheaths at the

two electrodes cannot be equaled. This leads that the sheath at one of the two electrodes overcomes to other. At this condition the nonlinearity will be very clear, this situation attributes to the asymmetry discharge condition. When the angle is larger than the limit mentioned formerly above, this leads a new effect to be appear. The discharge will stop between all electrodes surface area, but occurs between all smaller electrodes surface area and a part surface area from the larger electrode, which represents a geometrical symmetry for the smaller electrode. As a result from this condition the discharge back to electrically symmetry from the situation of the asymmetric discharge. In this case the nonlinearity components decreased, which are related to asymmetry discharge. The increasing in the angle at this condition leads to release the plasma toward the wall of the plasma container and the discharge occurs indirectly between the two electrodes during the wall of the discharge container. In this case the nonlinearity is very high. The distortion in the current wave produces by the second harmonic associated with the fundamental frequency because the other harmonics will be very small effect compared with the second harmonic [14]. Experimental study of the DC and second harmonic contents in 13.56 RF glow discharge indicated to the association property of these two components. The argument for these words, researches recently work in this field used two frequencies applied on the symmetrical geometry capacitively coupled discharge plasma fundamental frequency 13.56 MHz and its harmonic 27.12 MHz as a *df ccrf* discharge. During the tuning for the two phase angles for the two Rf voltage applied lead to control of the DC bias, Heil et al., [19] found that the DC bias is a nearly linear function with the phase angle. Schungel [22] proved the same result of Heil et al., [19] experimentally, but with the asymmetric *df ccrf* discharge by using applied voltages with frequencies 13.56 MHz and its harmonic 27.12 MHz, and denotes that the DC bias is as a function of the phase angle (phase shift), but its absolute value is strongly affected by the electrode area ratio.

Conclusions

From above one may conclude the following:

The DC and second harmonic contents in 13.56 RF glow discharge indicated the association property of these two components. The results indicated significant increase in distortions at two specific values of the cone angle enclosing the two electrodes within its geometrical volume. The systematic is increasing for these components with all RF powers. The computation of the cone head angle gave the symmetry discharge or asymmetry. When the angle is small the condition is near symmetry discharge associated with decrease in the nonlinearity. When the angle was increasing to a specific value the property of the nonlinearity is increases very clear.

Acknowledgment

I would like to express my deep appreciation Prof. Aasim Azooz for his help in this work. The help of the head and staff of the physics department are also highly valued.

References

[1] B. Chapman: Glow Discharge Process (Johan Wiley & Sons, New York, (1980) Ed., 144-159).

[2] Yu. P. Raizer, M. N. Schneider, N. A. Yatsenko: Radio-frequency capacitive discharge (CRC Press London, (1995) Ed., 111-131).

[3] M. A. Liebermann and A. J. Lichtenberg: Principles of Plasma Discharges and Materials Processing (Wiley & Sons, (1994) Ed., 328-385).

[4] P. Chabert and N. St. J. Braithwaite: Physics of radio-frequency plasmas (Cambridge University Press, New York, (2011) Ed., 131-175).
[5] V. A. Godyak, R. B. Piejak, and B. M. Alexandrovich, J. Appl. Phys. 61 (1990) 2401-2406.
[6] V. A. Godyak, R. B. Piejak, and B. M. Alexandrovich, IEEE Trans. on Plasma Sci. 19 (1991) 660-676.
[7] V. A. Lisovskiy, J.P. Booth, K. Landry, D. Douai, V. Cassagne, and V. D. Yegorenkov, IEEE Trans. on Plasma Sci. 35, 2 (2007) 416-424.
[8] R. A. Gottscho, G. R. Scheller, D. Stoneback, and T. Intrator, J. Appl. Phys. 66 **(**1989**)** 492-500.
[9] M. A. Sobolewski, IEEE Trans. Plasma Sci. 23(1995) 1006–1022.
[10] D. Gahan, S. Daniel, C. Hayden,P. Scullin, D. O. Sullivan, Y. T. Pei and M. B. Hopkins, J. Plasma Sources Sci. Technol. 21(2012) 1-8.
[11] M. A. Ahmad, Iraqi Journal of Physics 10,17 May(2012) 90.
[12] H. Kawata, T. Kubo and K. Murata, Jpn. J. Appl. Phys. 33(1994) 4365-4368.
[13] P. Linardaki, and G. G. Borg, IEEE Mic. And Wireless Components Lett. 18 (2008)164-166.
[14] J. Asmussen and Q. H. Lee, Appl. Phys. Lett. 15 (1969) 182-186.
[15] M. N. A. Dewan and P. J. McNally, J. Appl. Phys. 91(2002) 5604-5613.
[16] M. A. Lieberman,: IEEE Trans. on Plasma Sci. 16(1988) 638-644.
[17] M. A. Lieberman, J. Appl. Phys. 65 (1989) 4186- 4191.
[18] M. S. Barnes, T. J. Colter and M. E. Elta, J. Appl. Phys. 61(1987) 81-89.
[19] B. G. Heil, U. Czarnetzki, R. P. Brinkmann and T. Mussenbrock, J. Phys. D: Appl. Phys. 41(2008) 1-19.
[20] A. Azooz, Instruments and Experimental Techniques, 54, 3 (2011) 364–368.
[21] R. T. Hilbish, R. M. Montgomery and R. A. Holmes, J. Appl. Phys. 39 (1968) 5782-5791.
[22] E. Schungel, D. Eremin, J. Schulze, T. Mussenbrock, U. Czarnetzki, J. Appl. Phys. 112 (2012) 1-13.